



Cite this: DOI: 10.1039/d5sc02212f

All publication charges for this article have been paid for by the Royal Society of Chemistry

# Divergent reactivity of intramolecular cycloadditions of keteniminium ions with alkynes: [4+2] or [2+2]?†

Sangjun Lee and Thomas R. Hoye \*

We describe here divergent reactivity in the intramolecular cyclizations of a family of keteniminium ions (KIs) that contain a tethered alkyne. The KI precursors were tertiary amides having (i) unsaturation (arene or alkene) located  $\beta,\gamma$  to the amide carbonyl and (ii) an alkyne tethered through the amide nitrogen atom. The KIs were generated by the action of triflic anhydride and a pyridine base at 0 °C. Substrates having a three-atom linker between the central carbon atom of the KI undergo unprecedented [4 + 2] cycloadditions between the alkyne and the styrenic/dienic subunit of the conjugated KI leading to indoline or carbazole derivatives. DFT computations suggest that the reaction proceeds by a stepwise mechanism. In contrast, substrates with a four- or five-atom tether undergo [2 + 2] cycloaddition to afford isolable, fused, cyclobutenyl iminium ions further useful as synthons.

Received 22nd March 2025  
Accepted 11th July 2025

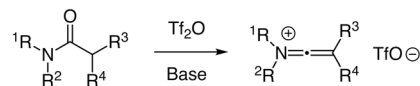
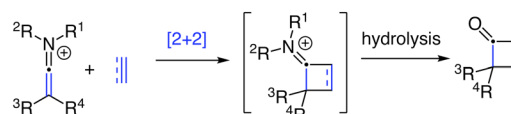
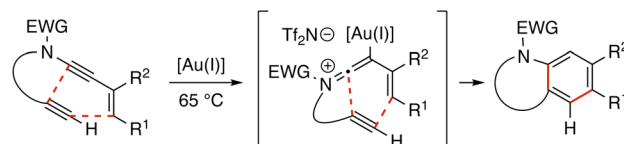
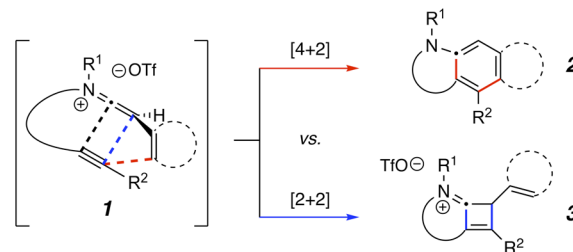
DOI: 10.1039/d5sc02212f

rsc.li/chemical-science

## Introduction

Keteniminium ions (KIs), quaternized nitrogen analogs of ketenes, have attracted much attention because of their inherently high reactivity.<sup>1</sup> After the development of *in situ* generation of KIs from tertiary amides (Fig. 1a), largely popularized by Ghosez and co-workers,<sup>2</sup> a variety of additional types of reactions that engage the KI have been reported. In particular, electrophilic KIs can react with a broad range of nucleophiles as well as participate in cycloaddition processes with electron-rich,  $\pi$ -functional groups. The latter include many examples of [2 + 2] cycloadditions with alkenes in both inter- and intramolecular fashion.<sup>3</sup> Although rare, a KI engaging a 1,3-diene in a [4 + 2] cycloaddition is known.<sup>4</sup> Also rare is the reaction between a KI and an alkyne in a [2 + 2] mode to produce a cyclobutenone (following hydrolytic workup of an initially formed iminium ion; Fig. 1b).<sup>2,5</sup>

The only example we can identify of a KI-like species engaging an alkyne in an intramolecular cycloaddition is the Au(I)-catalyzed process depicted in Fig. 1c.<sup>6</sup> In the studies we describe here (Fig. 1d), various amide precursors of the KI triflates **1** bearing a tethered alkyne have been shown to undergo either [4 + 2] or [2 + 2] cycloadditions to produce fused aromatic compounds **2** or fused cyclobutene-containing products **3**, depending on the nature of the tether and the substituents present in **1**.

**a** Ghosez, 1981**b** Cycloaddition of KI with alkene (or alkyne, although rare)**c** Au-catalyzed formal dehydro-Diels-Alder reaction (via a KI intermediate)**d** This work: KI with tethered alkyne can do either [4+2] or [2+2]

**Fig. 1** (a) Keteniminium triflates from the reaction of tertiary amides with  $\text{TiF}_2\text{O}$ . (b) Cycloaddition of KIs to produce four-membered carbocycles. (c) A lone example of an intramolecular trapping of a KI-like species by a tethered alkyne. (d) Intramolecular cycloadditions of amide-derived KIs.

Department of Chemistry, University of Minnesota, 207 Pleasant St. SE., Minneapolis, Minnesota 55455, USA. E-mail: hoye@umn.edu

† Electronic supplementary information (ESI) available: Details of all experimental procedures used to prepare new chemical entities (NCEs); line listings of spectroscopic characterization data for all NCEs; copies of all  $1\text{D } ^1\text{H}$ ,  $^{13}\text{C}$ , and  $^{19}\text{F}$  NMR spectra as well as selected sets of 2D NMR data; Excel file of the shielding tensors used in the DP4+ analysis of **22**. See DOI: <https://doi.org/10.1039/d5sc02212f>

## Results and discussion

In an early experiment in the studies we are reporting here, the arylalkyne-bearing tertiary amide **4a** was treated at 0 °C with triflic anhydride (Tf<sub>2</sub>O) and 1.1 equivalents of 2-iodopyridine (Fig. 2a), following the lead of Maulide and coworkers on the choice of base.<sup>7</sup> The amide **4a** was consumed within 10 minutes and the 2,3-dihydro-1*H*-benzo[*f*]indole (referred to hereafter as

simply an indoline) derivative **7a-H<sup>+</sup>** was generated and isolated in 80% yield following a quench with NaHCO<sub>3</sub>. This product presumably arises through the intermediacies of the KI **5** and its [4 + 2] Diels–Alder adduct **6**, which upon proton loss to aromatize the naphthalene moiety and reprotonation at N1 gave **7a-H<sup>+</sup>** before the NaHCO<sub>3</sub> quench. A similar experiment was carried out in CDCl<sub>3</sub> solution. The *in situ* <sup>1</sup>H NMR spectrum prior to any workup (Fig. 2b) indicated that the protonated

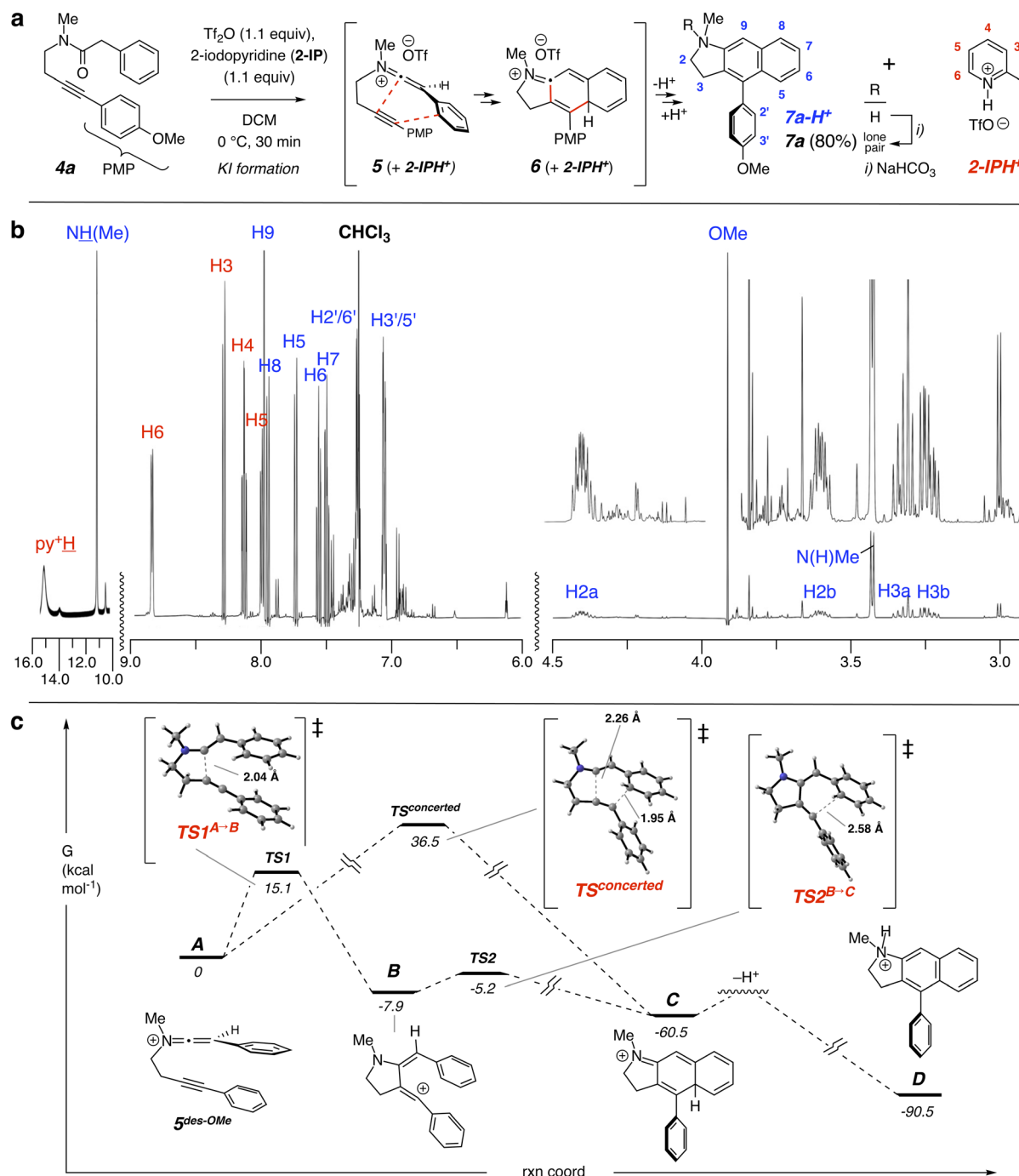


Fig. 2 Reaction of **4a** with Tf<sub>2</sub>O and 2-IP produced, upon workup and isolation, the indoline derivative **7a**: (a) the balanced equation and postulated intermediates, (b) an *in situ* <sup>1</sup>H NMR spectrum of the reaction mixture in CDCl<sub>3</sub>, and (c) DFT\* energies for the PES of A to D suggest a stepwise cycloisomerization of A to C. \*ωB97X-D/def2-SVP/SMD(DCM).<sup>11</sup>

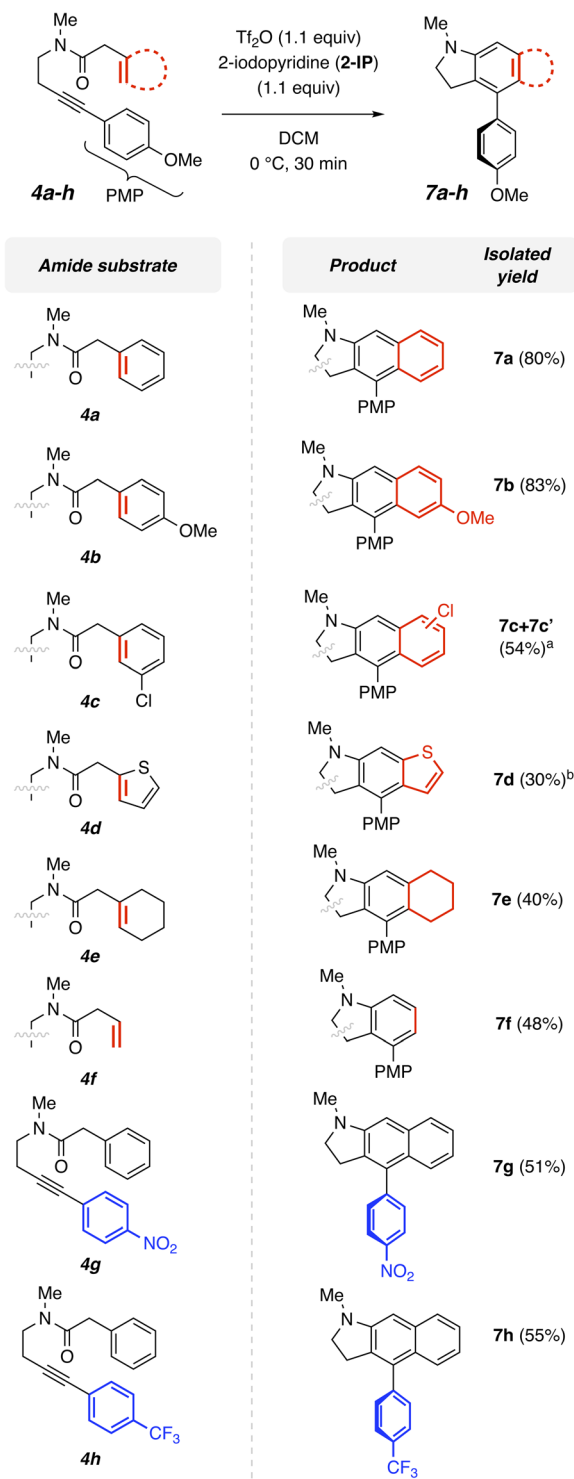


Fig. 3 Reactions of amides (**4a–4h**) with  $\text{Tf}_2\text{O}$  and 2-IP to produce indolines (**7a–7h**), respectively. <sup>a</sup>Inseparable regioisomers were isolated (~1 : 1). <sup>b</sup>0 °C, 10 min to rt, 2 h.

indolinium species **7-H<sup>+</sup>** (note the methyl doublet at 3.4 ppm) and iodopyridinium triflate ions were, by far, the major components present, accounting for the fate of the two equivalents of triflic acid that are the requisite byproducts<sup>8</sup> of the reaction.

Although DFT studies have been reported for cycloaddition reactions of KIs with alkenes or electron rich heterocycles,<sup>4b,9</sup> analogous computational investigations involving reactions of KIs with alkynes are more limited.<sup>10</sup> Using methodology<sup>11</sup> that has proven to be effective in some of the above studies,<sup>9b–d</sup> we carried out DFT calculations starting with species **5<sup>des-OMe</sup>** (=state **A**, Fig. 2c), a slightly simplified (and computationally more tractable) analog of the anisole-containing KI **5**, to explore the net cycloaddition event(s) that convert(s) **5** to **6**. A concerted transition state (TS) for a single step process that directly produces **C** was identified, but the activation barrier (36.5 kcal mol<sup>-1</sup>) for its formation was excessively high for that to be likely. Alternatively, a stepwise sequence converting **A** to the cationic intermediate **B** was seen to have a low barrier (15.1 kcal mol<sup>-1</sup>) and, further, to easily close the second CC-bond to produce **C**. The aromatized isomeric indolinium ion **D** was, not surprisingly, considerably more stable than **C**.

Encouraged by these initial results, we expanded our investigations with substrates having different aryl (**4b–d**) or alkenyl (**4e–f**) substituents alpha to the amide carbonyl group to test the compatibility of different  $\pi$ -systems in the [4 + 2] cycloaddition reaction (Fig. 3). First, replacing the electron-neutral aryl in **4a** with an electron-donating *p*-methoxyphenyl (PMP) group in **4b**

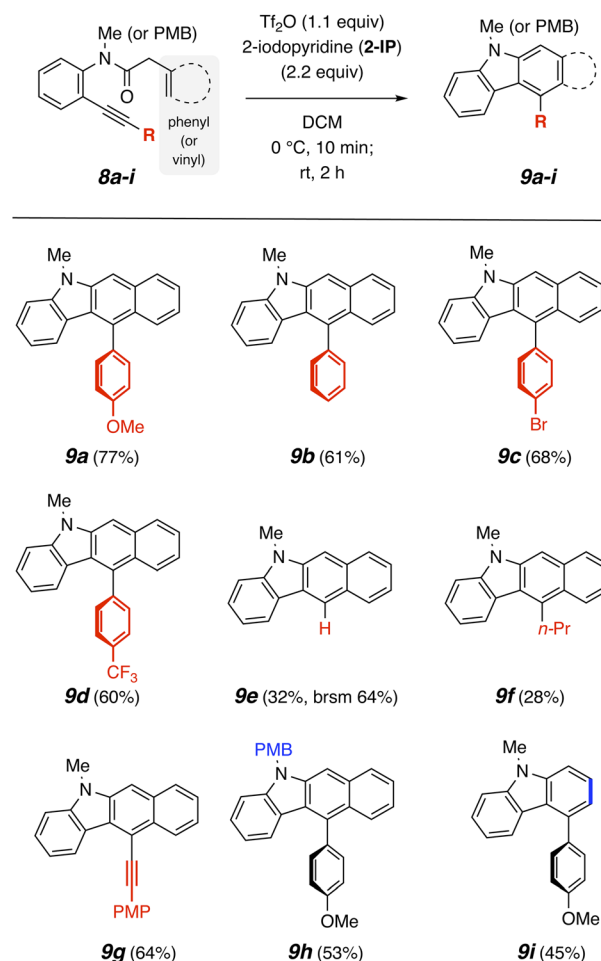


Fig. 4 Reactions of amides (**8a–8i**) with  $\text{Tf}_2\text{O}$  and 2-IP afford carbazoles (**9a–9i**).

generated the indoline **7b** in 83% yield. The relatively electron-deficient (and desymmetrized) *m*-chlorophenyl (MCP) substituent in **4c** also led to the formation of the indoline ring, now as a mixture of **7c** and **7c'** (*ca.* 1 : 1 ratio). This bifurcation occurs at the stage of an analog of **5** (Fig. 2a), which now has two different ortho carbon atoms at C2 and C6 of its unsymmetrical MCP substituent. Thiophene also participated in the [4 + 2] cycloaddition event as shown by the formation of **7d**. Non-aryl  $\pi$ -systems were also compatible with the process: a substrate having a cyclohexenyl (*viz.* **4e**) or a vinyl (*viz.* **4f**) group produced **7e** or **7f**, respectively, in modest yield. Substrates **4g** and **4h** having electron-deficient arene substituents at the alkyne terminus were examined. They afforded **7g** and **7h** in comparable yields. These results suggest that the electronic nature of the aryl-alkyne substituent does not significantly impact the reaction outcome.

We have also examined a series of substrates in which the ethano-linker in **4** was replaced by a benzo-linker as seen in **8a–i**. Reactions of these amides afforded carbazole derivatives as products (Fig. 4). In all of these reactions, use of two equivalents of **2-IP** was advantageous, presumably because the carbazole product was not sufficiently basic to efficiently maintain an effective portion of the pyridine free base. The tolerance for the R-group in substrates **8a–i** was probed and the corresponding products **9a–i** were obtained, albeit in marginal yields for (the desilylated) **9e** and alkyl substituted **9f**. The compatibility of two additional variations is shown by the formation of (i) the *N*-PMB analog **9h** from **8h** and (ii) the parent carbazole **9i** from engagement of the simple vinyl group in the 3-butenyl amide **8i**.

We next hypothesized that increasing the length of the tether between the amide carbonyl and alkyne would bias the nature

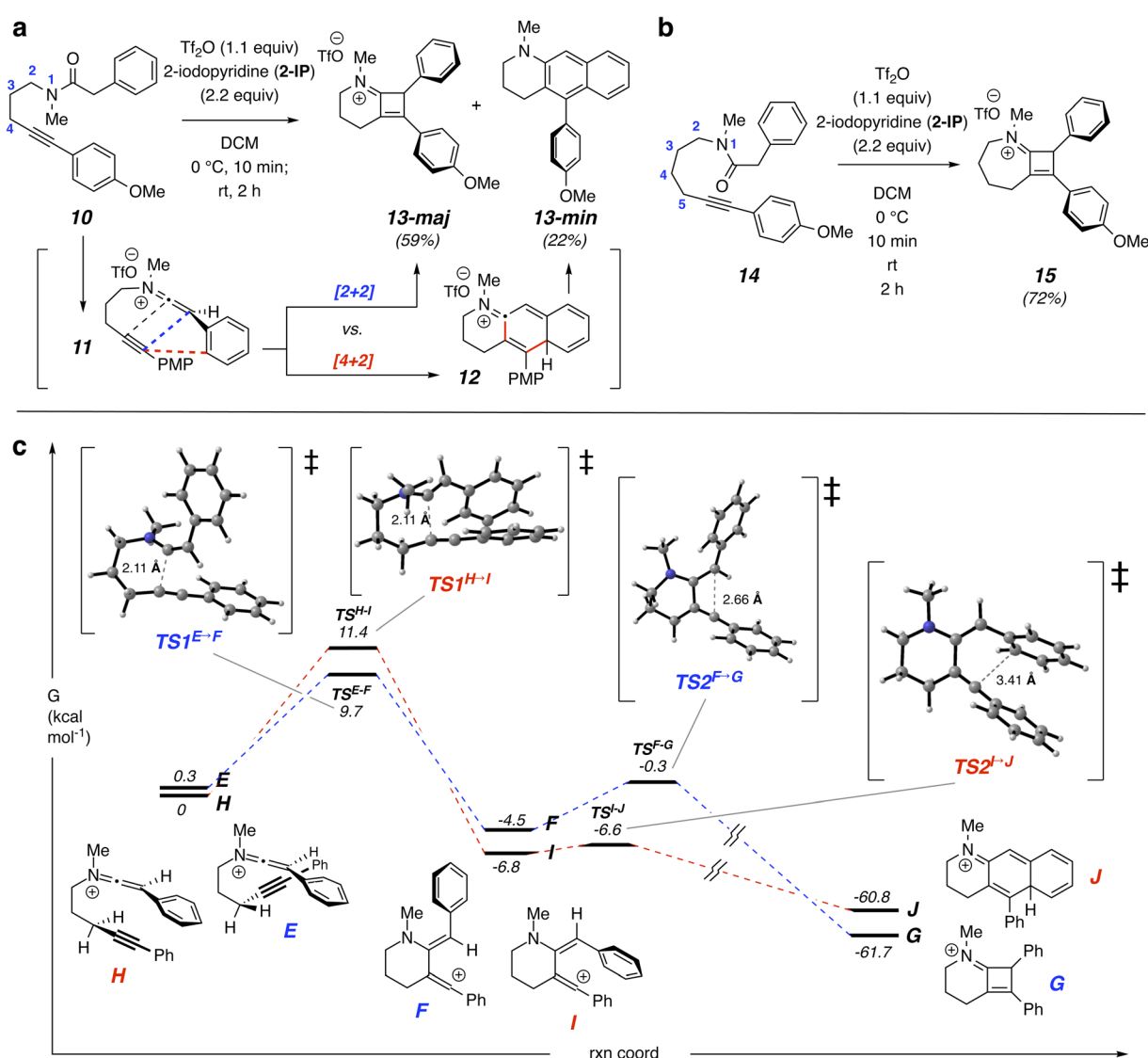


Fig. 5 Reactions of amides **10** and **14**, having different length tethers between the amide and alkyne units, with  $\text{Ti}_2\text{O}$  and 2-IP. (a) The substrate with a trimethylene tether provides **13-maj** and **13-min** via competitive [2 + 2] and [4 + 2] cycloadditions, respectively. (b) The substrate with a tetramethylene tether exclusively affords the 7/4 bicyclic iminium ion **15** via the [2 + 2] pathway. (c) DFT\* indicates that the competition leading to **13-maj** vs. **13-min** occurs in the initial bond forming events (*cf.*  $\text{TS}^{\text{E} \rightarrow \text{F}}$  vs.  $\text{TS}^{\text{H} \rightarrow \text{I}}$ ). \* $\omega\text{B97X-D/def2-SVP/SMD(DCM)}^{11}$ .

of the cycloisomerization event (*cf.* examples of this phenomenon in HDDA<sup>12a</sup> and PDDA reactions<sup>12b</sup>) to favor a [2 + 2] rather than [4 + 2] mode of cycloaddition. Reaction of substrate **10**, which has a trimethylene linkage between the amide and alkyne nitrogen atom, led to the formation of **13-maj** and **13-min**, isolated in good yield following chromatographic separation (Fig. 5a). That is, formation of the bicyclic iminium ion **13-maj** from KI **11** is now the preferred reaction mode. Although it was no longer the predominant pathway, the [4 + 2] event within **11** to give **13-min** was still significant. This result shows that the length of the linkage between the KI and alkyne plays an important role in influencing the reactivity of intramolecular cycloaddition. This begged the question of how the homologous tetramethylene substrate **14** would behave. It provided the 7/4 bicyclic iminium ion **15** *via* [2 + 2] cycloaddition as the only isolable product in 72% yield; none of the [4 + 2] isomeric product was detected in the <sup>1</sup>H NMR spectrum of the crude product mixture.

To rationalize the two competing reaction pathways from **10** to **13-maj** (*via* [2 + 2]) and **13-min** (*via* [4 + 2]), a DFT calculation was performed using the (slightly simpler) phenyl analog of the KI **11** (Fig. 5c). This KI was shown to have the *syn*- and *anti*-geometries depicted as the conformers **E** and **H**, respectively, as the two lowest energy conformers. These were nearly equi-energetic and can be expected to readily interconvert. Each proceeded to the corresponding vinyl carbocations **F** and **I**, respectively, through **TS1<sup>E→F</sup>** and **TS1<sup>H→I</sup>** (confirmed by IRC analysis). Products **F** and **I**, differ in the *Z*-vs. *E*-geometry of their aminoalkene. Structure **F** was seen to proceed to the [2 + 2]-adduct **G**, and **I** to the [4 + 2]-adduct **J**; each of these steps had a very low activation barrier. Thus, the rate-limiting and, therefore, product-determining primary event on these parallel, competitive reaction processes is determined by the relative Gibbs energies of the transition structures **TS1<sup>E→F</sup>** and **TS1<sup>H→I</sup>**; the former, which commits the KI to the formation of the [2 + 2]-adduct, is 1.7 kcal mol<sup>−1</sup> lower. The bottom line is that this DFT analysis indicates that it is reasonable that the formation of both the 4-membered and 6-membered ring-containing products **13-maj** and **13-min** is competitive within **11**.

With the insight from DFT that the reaction of **10** can proceed competitively to form isomeric intermediate vinyl cations having either *E*- or *Z*-geometry in the appended enamine, we computed the analogous pairs of possible TSs for each of the (des-methoxy) KIs derived from **14** and **4a** (*i.e.*, **5<sup>des-OMe</sup>**). The details of these results are provided in Fig. S4 in the ESI.† For the case of the three-atom tethered amide **4a**, the computed  $\Delta\Delta G^\ddagger$  for **5<sup>des-OMe</sup>** favored the formation of the *E*-enamine, the precursor to the 6-membered [4 + 2] product, by 1.0 kcal mol<sup>−1</sup>. For the case of the five-atom tethered amide **14**, the computed  $\Delta\Delta G^\ddagger$ s of the two TSs favored the formation of the *Z*-enamine intermediate, the precursor to the [2 + 2] product, by 2.0 kcal mol<sup>−1</sup>, a value (slightly) higher than that for the case of **TS1<sup>E→F</sup>** *vs.* **TS1<sup>H→I</sup>** (Fig. 5c). Although the energetics of these computed  $\Delta\Delta G^\ddagger$ s (−1.0, 1.7, and 2.0 kcal mol<sup>−1</sup>) for the three amide substrates do not perfectly map onto the observed product ratios, they certainly do mirror the trend of the

experimental results (*i.e.*, [4 + 2] only from **4a**; both [4 + 2] and [2 + 2] from **10**; [2 + 2] only from **14**).

To explore some of the potential that these cyclobutene-containing [2 + 2] cycloadducts might have for serving as building blocks of value in synthesis,<sup>13</sup> we prepared amide **16** possessing removable PMB and TMS groups (Fig. 6). This amide underwent [2 + 2] cycloaddition smoothly and with excellent yield to give only the iminium ion **17**; no [4 + 2] product was observed in the <sup>1</sup>H NMR spectrum of the crude product mixture. Treatment of **17** or **13-maj** with aqueous sodium hydroxide smoothly gave the cyclobutenone<sup>14</sup> **18** or **19**, respectively (*cf.* Fig. 1b). Each of these amines was more readily purified upon conversion to its respective acetamide derivative **18-Ac** or **19-Ac**.

Upon reduction of **17** with sodium borohydride at room temperature in an attempt to produce the bicyclic amine **20**, we instead obtained a crude product whose <sup>1</sup>H NMR spectral data suggested it to be, mostly, the diene **21**. This material was directly subjected to treatment with *N*-methylmaleimide (4

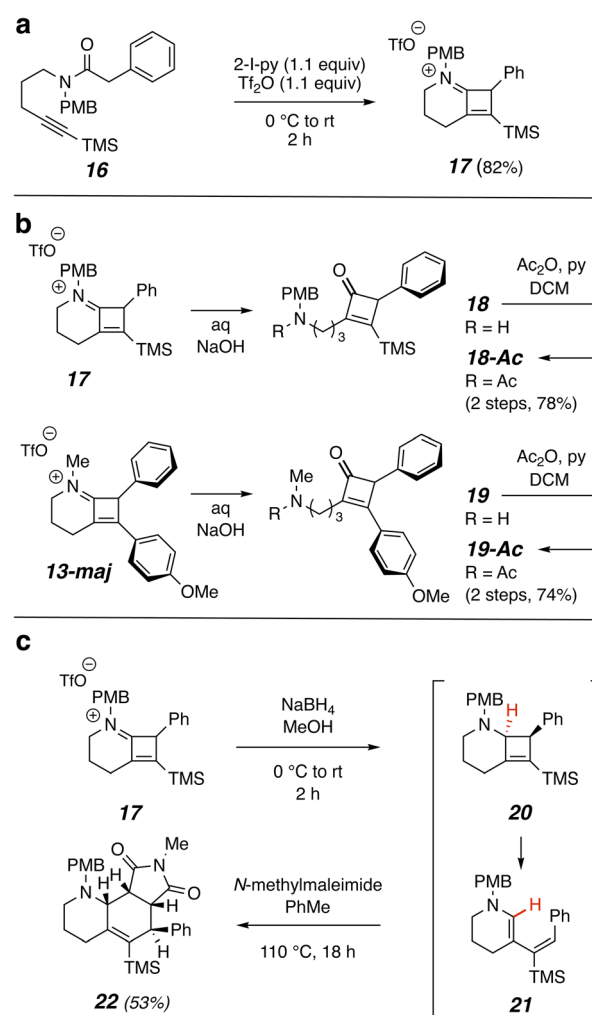


Fig. 6 Derivatization of cyclobutene-containing bicyclic iminium ions. (a) [2 + 2] Cycloaddition of the amide **16** with two protecting groups (1 mmol scale). (b) Hydrolysis of the bicyclic iminium ions **17** and **13-maj** to form cyclobutenone derivatives **18** and **19**, followed by acylation. (c) Cascade of iminium ion reduction, 4 $\pi$ -electrocyclic ring-opening, and Diels–Alder reaction of **17** leading to **22** (*via* **20** and **21**).



equiv). This mixture required heating at 110 °C for multiple hours to achieve full consumption of the diene. The product of this Diels–Alder reaction, the hydroquinoline derivative **22**,<sup>15</sup> was obtained in 53% yield following purification. The relative configuration of this compound was established by careful analysis of the NMR features of the four methine protons on the newly formed cyclohexene moiety. Four possible diastereomers were considered; namely, those arising from either endo- or exo-addition of either the *E*- or *Z*-trisubstituted alkene in **21**. These four were evaluated in a DP4+ analysis,<sup>16</sup> which compared the computed NMR chemical shifts with the experimentally determined values (see the ESI† for details). This gave a 100% probability that the structure of this adduct was as shown in **22**. Backward deduction indicates (i) that the diene **21** was the indicated *E*-isomer and (ii) that the intermediate **20** was selectively produced in the hydride reduction. Conrotatory electrocyclic opening of **20** resulted in **21**.<sup>17</sup> Searching the literature suggested (i) that dienes having the *Z*-geometry but otherwise analogous features to those of **21** undergo DA cycloadditions with maleimides quite readily (*e.g.*, ≤25 °C) but (ii) that dienes having analogous structures to that of **21** often require temperatures >100 °C to allow for convenient reaction times. One particularly relevant example of this in the literature showed analogous coupling constant data for a set of similarly arranged, four methine protons.<sup>18</sup>

## Conclusion

We have discovered two distinct modes of intramolecular reactivity of conjugated KIs with alkynes: [4 + 2] and [2 + 2] cycloadditions. These different reactivities are largely dictated by the length of the tether between the KI and alkyne. First, a three-atom tether leads to unprecedented [4 + 2] cycloaddition reactivity at ambient temperature. Depending upon the nature of the tether and substituents present in the (readily constructed) amide precursors, production of a variety of indoline and carbazole derivatives was achieved. DFT studies using the KI **A**, having a three-atom tether between the alkyne and electrophilic carbon atom, indicated that a stepwise pathway that initially closes to a vinyl cation has a significantly lower activation barrier than a concerted process for the net [4 + 2] cycloaddition process ( $E_{\text{act}} = 15.1$  vs. 36.2 kcal mol<sup>−1</sup>, respectively). We also showed that net [2 + 2] cycloaddition became progressively more dominant as the length of the tether was increased from 3 to 4 to 5 atoms. A parallel DFT analysis of the KI **E/H** having a four-atom tether gave energetics consistent with the competitive formation of the [2 + 2]- and [4 + 2]-cycloadducts **13-maj** and **13-min** from **10**. Analogous DFT computations for amides **4a** and **14** showed a correlation between the  $\Delta\Delta G^\ddagger$  values for the formation of *Z*- vs. *E*-enamine intermediates and the observed preference for forming products *via* the [4 + 2] vs. [2 + 2] pathways. This suggests that DFT would be a useful tool in aiding the design of new tether structures aimed at providing either six- or four-membered products from intramolecular KI cycloadditions.

Finally, we demonstrated the derivatization of isolable and novel bicyclic cyclobutenyl iminium ions. Hydrolysis furnished

amino-substituted cyclobutenone derivatives. Reduction of the iminium ion gave a transient aminocyclobutene, which generated a diene *via* a low-barrier 4 $\pi$ -electrocyclic ring-opening. This diene subsequently underwent a Diels–Alder reaction with *N*-methylmaleimide to give an sp<sup>3</sup>-rich polycycle, the relative configuration of which was elucidated by DP4+ NMR analysis. This indicated that the hydride reduction of the precursor iminium ion was highly diastereoselective and that conrotatory pericyclic ring opening had provided the *E*-alkene isomer.

## Data availability

The data used to support the conclusions described in this manuscript are provided either in the ESI† document or in a master Mnova file (.zip) of all NMR spectra.

## Author contributions

S. L. conceived the project, performed the experiments, characterized all new compounds, and performed the DFT computations. S. L. and T. R. H. interpreted the data and co-wrote the manuscript.

## Conflicts of interest

There are no conflicts to declare.

## Acknowledgements

This research was supported by a grant from the National Institutes of General Medical Sciences (R35 GM127097) of the United States National Institutes of Health (NIH). NMR data were collected with an instrument funded in part by the Shared Instrumentation Grant program (S10 OD011952) of the NIH. ESI HRMS data were obtained at the Analytical Biochemistry Shared Resource laboratory in the Masonic Cancer at the University of Minnesota using an instrument that was partially funded by a Cancer Center Support Grant (P30 CA77598) from the NIH. The DFT computations were done using facilities at the University of Minnesota Supercomputing Institute (MSI). We are appreciative of helpful conversations about DFT computations with Dr Jorge Barroso and Prof. Melissa Ramirez.

## Notes and references

- (a) L. Ghosez and J. Marchand-Brynaert, Iminium salts in organic chemistry, Part I, in *Advances in organic chemistry*, ed. H. Böhme and H. G. Viehe, H. G. Wiley, New York, 1976, pp. 421–532; (b) C. Madelaine, V. Valerio and N. Maulide, Revisiting keteniminium salts: more than the nitrogen analogs of ketenes, *Chem.-Asian J.*, 2011, **6**, 2224–2239; (c) G. Evano, M. Lecomte, P. Thilmany and C. Theunissen, Ketiminium ions: unique and versatile reactive intermediates for chemical synthesis, *Synthesis*, 2017, **49**, 3183–3214.
- J. Falmagne, J. Escudero, T. Taleb-Sahraoui and L. Ghosez, Cyclobutanone and cyclobutenone derivatives by reaction



- of tertiary amides with alkenes or alkyne, *Angew. Chem., Int. Ed.*, 1981, **20**, 879–880.
- 3 B. B. Snider, Intramolecular cycloaddition reactions of ketenes and keteniminium salts with alkenes, *Chem. Rev.*, 1988, **88**, 793–811.
  - 4 (a) F. Mahuteau-Betzer, P. Ding and L. Ghosez, First [4+2] cycloadditions involving the olefinic bond of an 'aldoketeniminium salt' (=N-Alk-1-enylideneaminium salt), *Helv. Chim. Acta*, 2005, **88**, 2022–2031; (b) M. Ramirez, W. Li, Y. Lam, L. Ghosez and K. N. Houk, Mechanisms and conformational control of (4 + 2) and (2 + 2) cycloadditions of dienes to keteniminium cations, *J. Org. Chem.*, 2020, **85**, 2597–2606.
  - 5 A. Lumbroso, S. Catak, S. Sulzer-Mossé and A. De Mesmaeker, Cycloaddition of keteniminium with terminal alkynes toward cyclobuteniminium and their use in Diels-Alder reactions, *Tetrahedron Lett.*, 2014, **55**, 5147–5150.
  - 6 Q. Zhao, D. F. L. Rayo, D. Campeau, M. Daenen and F. Gagosz, Gold-catalyzed formal dehydro-Diels-Alder reactions of ene-ynamide derivatives bearing terminal alkyne chains: scope and mechanistic studies, *Angew. Chem., Int. Ed.*, 2018, **57**, 13603–13607.
  - 7 D. Kaiser, A. de la Torre, S. Shaaban and N. Maulide, Metal-free formal oxidative C-C coupling by in situ generation of an enolonium species, *Angew. Chem., Int. Ed.*, 2017, **56**, 5921–5925.
  - 8 W. Watson, On byproducts and side products, *Org. Process Res. Dev.*, 2012, **16**, 1877.
  - 9 (a) W.-J. Ding and D.-C. Fang, Theoretical studies on cycloaddition reactions between keteniminium cations and olefins, *J. Org. Chem.*, 2001, **66**, 6673–6678; (b) M. A. Maskeri, A. J. Fernandes, G. D. Mauro, N. Maulide and K. N. Houk, Taming keteniminium reactivity by steering reaction pathways: computational predictions and experimental validations, *J. Am. Chem. Soc.*, 2022, **144**, 23358–23367; (c) P. Zhang and Z.-X. Yu, Kinetic, thermodynamic, and dynamic control in normal vs. cross [2 + 2] cycloadditions of ene-keteniminium ions: computational understanding, prediction, and experimental verification, *J. Am. Chem. Soc.*, 2023, **145**, 9634–9645; (d) P. Zhang and Z.-X. Yu, Dynamically or kinetically controlled? computational study of the mechanisms of electrophilic aminoalkenylation of heteroaromatics with keteniminium ions, *J. Org. Chem.*, 2024, **89**, 4326–4335.
  - 10 L. R. Domingo, M. Ríos-Gutierrez and P. Perez, A DFT study of the ionic [2+2] cycloaddition reactions of keteniminium cations with terminal acetylenes, *Tetrahedron*, 2015, **71**, 2421–2427.
  - 11 (a) J. D. Chai and M. Head-Gordon, Long-range corrected hybrid density functionals with damped atom-atom dispersion corrections, *Phys. Chem. Chem. Phys.*, 2008, **10**, 6615–6620; (b) F. Weigend and R. Ahlrichs, Balanced basis sets of split valence, triple zeta valence and quadruple zeta valence quality for H to Rn: Design and assessment of accuracy, *Phys. Chem. Chem. Phys.*, 2005, **7**, 3297–3305.
  - 12 (a) X. Xiao, B. P. Woods, W. Xiu and T. R. Hoye, Benzocyclobutadienes: an unusual mode of access reveals unusual modes of reactivity, *Angew. Chem., Int. Ed.*, 2018, **57**, 9901–9905; (b) Q. Xu and T. R. Hoye, Electronic character of  $\alpha$ ,3-dehydrotoluene intermediates generated from isolable allenyne-containing substrates, *Angew. Chem., Int. Ed.*, 2022, **61**, e202207510.
  - 13 J. W. Greenwood, M. A. Larsen, S. A. Burgess, J. A. Newman, Y. Jiang and A. C. Sather, Isolable iminium ions as a platform for N-(hetero)aryl piperidine synthesis, *Nat. Synth.*, 2023, **2**, 1059–1067.
  - 14 (a) P. Chen and G. Dong, Cyclobutenones and benzocyclobutenones: versatile synthons in organic synthesis, *Chem.-Eur. J.*, 2016, **22**, 18290–18315; (b) L. Deng, T. Xu, H. Li and G. Dong, Enantioselective Rh-catalyzed carboacylation of C=N bonds via C-C activation of benzocyclobutenones, *J. Am. Chem. Soc.*, 2016, **138**, 369–374; (c) X. Zhou, I. Zafar and G. Dong, Catalytic intramolecular decarbonylative coupling of 3-aminocyclobutenones and alkenes: a unique approach to [3.1.0]bicycles, *Tetrahedron Lett.*, 2015, **71**, 4478–4483; (d) S. Dutta, Y.-L. Lu, J. E. Erchinger, H. Shao, E. Studer, F. Schäfer, H. Wang, D. Rana, C. G. Daniliuc, K. N. Houk and F. Glorius, Double strain-release [2 $\pi$ +2 $\sigma$ ] photocycloaddition, *J. Am. Chem. Soc.*, 2024, **146**, 5232–5241.
  - 15 For selected examples of synthesis studies leading to hydroquinoline derivatives, see: (a) P. A. Grieco and D. T. Parker, Octahydroquinoline synthesis via immonium ion based Diels-Alder chemistry: synthesis of (–)-8a-epipumilotoxin C, *J. Org. Chem.*, 1988, **53**, 3658–3662; (b) A. Brosius, L. E. Overman and L. Schwink, Total synthesis of (+)-aloperine. Use of a nitrogen-bound silicon tether in an intramolecular Diels-Alder reaction, *J. Am. Chem. Soc.*, 1999, **121**, 700–709; (c) W. Aelterman and N. D. Kimpe, Synthesis of 3-vinylpiperidines, 3-ethylidenepiperidines and 5-functionalized-1,2,3,4-tetrahydropyridines, *Tetrahedron Lett.*, 1998, **54**, 2563–2574; (d) S. Kobayashi, K. Kudo, A. Ito, S. Hirama, T. Otani and T. Saito, The diene-transmissive hetero-Diels-Alder reaction of 2-vinyl  $\alpha,\beta$ -unsaturated aldimines: stereoselective synthesis of hexahydroquinazolin-2-ones, *Org. Biomol. Chem.*, 2014, **12**, 4061–4064; (e) K. Kanai, S. Kobayashi, K. Kudo, T. Honjo, T. Otani and T. Saito, An inverse electron-demand diene-transmissive hetero-Diels-Alder reaction of N-sulfonyl-[3]-1-azadendralenes for stereocontrolled synthesis of polyhydroquinolines, *Tetrahedron Lett.*, 2015, **56**, 5090–5093.
  - 16 N. Grimblat, M. M. Zanardi and A. M. Sarotti, Beyond DP4: an improved probability for the stereochemical assignment of isomeric compounds using quantum chemical calculations of NMR shifts, *J. Org. Chem.*, 2015, **80**, 12526–12534.
  - 17 For example, (a) A. G. Riches, L. A. Wernersbach and L. S. Hegedus, Synthesis of functionalized chiral (racemic) cyclobutanones, *J. Org. Chem.*, 1998, **63**, 4691–4696; (b) T. Gharbaoui, M. Legraverend and E. Bisagni, An efficient synthesis of 9-[(1-hydroxymethyl)-cyclobut-1-ene-3-yl]adenine and 1-(adenin-9-yl)-3-methylidene-but-1-ene-4-ol



via regiospecific addition of phenyl selenenyl bromide to the alkene precursor, *Tetrahedron Lett.*, 1992, **33**, 7141–7144; (c) Y. Xu, F. Tian and W. R. Dolbier, Synthetic and mechanistic aspects of the reaction of 1,1-difluoro-2,2-bis(dimethylamino)ethene with ethyl propiolate, *J. Org. Chem.*, 1999, **64**, 5599–5602.

18 D. C. G. A. Pinto, A. M. S. Silva, C. M. Brito, A. Sandulache, J. R. Carrillo, P. Prieto, A. Diaz-Oritz, A. de la Hoz and J. A. S. Cavaleiro, Reactivity of 3-styrylchromones as dienes in Diels–Alder reactions under microwave irradiation: a new synthesis of xanthenes, *Eur. J. Org. Chem.*, 2005, 2973–2986.

